Transmission through Highly Overdense Plasma Slabs with a Subpicosecond Relativistic Laser Pulse

J. Fuchs,[1,2] J. C. Adam,[3] F. Amiranoff,[2] S. D. Baton,[2] P. Gallant,[1] L. Gremillet,[2] A. Héron,[3] J. C. Kieffer,[1] G. Laval,[3] G. Malka,[4] J. L. Miquel,[4] P. Mora,[3] H. Pépin,[1] and C. Rousseaux[4]

[1]*INRS-Énergie et Matériaux, 1650 boulevard Lionel Boulet, J3X1S2 Varennes, Québec, Canada*

[2]*Laboratoire pour l'Utilisation des Lasers Intenses, CNRS, École Polytechnique, 91128 Palaiseau Cedex, France*

[3]*Centre de Physique Théorique, CNRS, École Polytechnique, 91128 Palaiseau Cedex, France*

[4]*Commissariat à l'Énergie Atomique, Limeil-Valenton, 94195 Villeneuve-Saint-Georges Cedex, France*

(Received 2 June 1997)

Transmission of a subpicosecond relativistic laser pulse is observed through solid foils and preformed overcritical plasmas. Transmission rates near 10% for densities above $10 \times n_c$ are measured. A moderately relativistic strong threshold in intensity is found in order to observe this effect. The experimental results as well as preliminary particle-in-cell simulations suggest that for thin solid foils the observed transmission is explicable by rapid heating and expansion to transmissive conditions during the pulse. Self-induced transparency and hole boring processes apply to thicker preformed plasmas. These results have important implications in fast ignition for inertial confinement fusion. [S0031-9007(98)05546-X]

PACS numbers: 52.40.Nk, 52.35.Mw, 52.60.+h, 52.70.Kz

For more than twenty years, overdense plasma interaction with laser pulses so intense that the oscillatory electron motion becomes relativistic has been a subject of much theoretical interest [1]. This interest has been considerably intensified, both theoretically [2,3] and experimentally [4,5], due partly to the availability of lasers capable of delivering intensities above 10^{19} W cm^{-2} [6] and partly to the advent of the fast ignitor concept [7] in the context of inertial confinement fusion. This scheme requires that a channeling [8] intense laser pulse penetrates as close as possible to the compressed core of the target. Classically, at low intensity, the normally incident light can propagate up to the critical density: $n_c = 1.1 \times 10^{21}/\lambda_\mu^2$ cm^{-3}, where λ_μ is the laser wavelength in microns. However, at high intensity, two mechanisms have been considered to allow wave propagation above n_c: (i) hole boring due to the ponderomotive pressure and (ii) self-induced transparency (SIT) due to the relativistic increase of the electron mass and the associated decrease of the effective plasma frequency, as observed both in 1D and 2D particle-in-cell (PIC) and fluid simulations [9,10].

In this context it is particularly important to study the currently unexplored propagation through moderately and very overdense layers. This is the object of the present Letter. We have explored a large set of plasma conditions: preformed overdense layers as well as solid foils. The experimental results, using a very high contrast beam, show that, at sufficiently high intensities, high transmission rates are attained for very overdense plasmas (with $n_{\max}/n_c \geq 10$). These transmissions decrease as the peak density or the overdense plasma thickness increases. The transmitted light is seen to originate from a small spot at the rear of the target. Moreover, the absorption appears to be relatively high ($\geq$50%) in the transmission regime. To our knowledge, this is the first time such results are reported. The preformed plasmas transmission results could possibly be interpreted in terms of the SIT and hole boring processes enhanced by self-focusing in the underdense corona. The thin solid foil results suggest the importance of target heating by fast electrons that leads to rapid expansion and density decrease to transmissive conditions during the pulse.

The experiments are performed with the 80 TW P102 laser system [6] at CEA/LV. A plasma-creating laser beam is focused by a $f/6$ lens through a random phase plate onto a CH or Al flat target, at 35° above the target normal. This 1.058 μm−750 ps FWHM laser pulse has an average intensity of $3\text{–}5 \times 10^{12}$ W/cm^2 (90% of 5 J contained in a 400 μm focal spot). After a time delay Δt, the subpicosecond high-intensity interaction beam is focused by a $f/3$ off-axis parabola at normal incidence onto the plasma with an energy up to 10 J ($\sim$20% of the energy being in the intense focal spot). By varying the delay between the creation pulse and the interaction pulse as well as the thickness of the target and the creation beam energy, it is possible to adjust the peak overdense density ($n_{\max}/n_c$) and the thickness at critical density (l_c). Two main configurations (referred systematically in the following as 2ω and 1ω) are used for the intense interaction beam: either the laser is frequency doubled at 529 nm and focused in the same direction as the creation beam, or it remains at 1.058 μm and is focused in the opposite direction. In both cases, the beam is linearly polarized, the pulse duration is 300–600 fs (FWHM), and the elliptical focal spots are rather close: either (2ω) 4×5 or (1ω) 5×10 μm^2. This leads to a maximum product $I\lambda^2$ of (2ω) 5 and (1ω) 15×10^{18} W cm^{-2} μm^2.

Transmission rates (through a $f/1.3$ lens) and reflection rates (in the $f/3$ focal aperture) of the intense beam are

 0031-9007/98/80(11)/2326(4)$15.00

measured using fast Hamamatsu photodiodes (100 ps rise time). We also monitor the outcoming beam by imaging the rear side of the target with a resolution of $\sim 0.5\ \mu$m.

Three Pockels cells having each a 10^3:1 contrast ratio and a rise time ~ 1 ns are used in the laser chain. At 1ω, this gives a repeated 10^8:1 contrast ratio for the continuum level up to -30 ps before the main pulse. On top of this continuum level two prepulses are measured at -350 and -30 ps; they present a contrast ratio of about 10^5 to 10^4:1. These contrast ratio measurements are done with a fast integrating diode up to -30 ps and with a third order autocorrelator from -35 to $+35$ ps. At 2ω, the contrast ratio is further squared by frequency doubling. It is thus much higher, better than 10^{12}:1 and 10^8:1 for the continuum and the prepulses, respectively. The residual energy at $1\ \mu$m is also reduced by at least a factor of 10^6 due to the 2ω coating reflective optics. With the 2ω peak intensity and contrast ratio, the intensity of the light prior to the main pulse is below the ionization threshold of solid targets. We studied the effect of the amplified spontaneous emission on solid targets by firing, at 2ω, a full energy shot without a pulse being injected in the regenerative amplifier. We did not observe any damage on the 700 Å Al foil after the shot. Because of the 1 ns rise time of the Pockels cells it is not possible to study the cumulative effects of the prepulses without the main pulse.

Nevertheless, in the case of the interaction with preformed plasmas we have verified both numerically and experimentally that the prepulses do not perturb the plasma produced by the creation beam. Using a Wollaston interferometer and a transverse diagnostic beam (0.35 μm, 1 ps), we get, by global Abel inversion, a 2D time-resolved measurement of the background density ~ 1 ps before the main pulse and with a spatial resolution better than 5 μm [8]. We do not record any perturbation due to prepulses. The measured background underdense density profiles ($n_e \leq 4 \times 10^{20}$ cm^{-3}) are fitted with a 1D Lagrangian hydrocode Chivas [11]. We can thus infer the $n_{\max}/n_c$ and l_c parameters. The density evolution of the target is very sensitive to the heat transport model used in the simulation. The best fit is obtained for a flux limit factor $f = (6 \pm 2)\%$. This variation of f gives a $\sim \pm 25\%$ variation on the peak density. Using a delocalized flux [12] is more relevant for the overdense part of the profiles except when the plasma becomes moderately overdense (a few tens of n_c). We chose the values of the peak density obtained with this heat transport model as the lower limit of the error bar [see Fig. 2(a)].

The density evolution given by the hydrocode is supported by monitoring the overdense/underdense peak density transition using the transmission of the creation beam and a time fiducial. The measured time at which the creation beam is transmitted through the plasma agrees well with the time at which the plasma becomes underdense in the hydrodynamic simulations using the flux limit factor model.

To be sure that the intense laser pulse is interacting with a high density plasma when using thin solid foils, we have used time-resolved x-ray spectroscopy (700 fs time resolution with the PX1 x-ray streak camera coupled to a conical crystal spectrometer viewing the plasma at 45° from the target normal). As an example a spectrum obtained by irradiating a 500 Å Al foil at 4.4×10^{18} W cm^{-2} μm^2 is shown in Fig. 1. The fit of the time-resolved Li-like spectrum [13] with line broadening calculations [14] indicates that the electron density, during the first 700 fs of the Li-like history, is around $2-5 \times 10^{23}$ cm^{-3} (solid density is 6×10^{23} cm^{-3}); this corresponds to $(50-125)n_c$. For $n_e < 2 \times 10^{23}$ cm^{-3} it is not possible to reproduce the observed spectra. From the extremely short duration of the Li-like emission (2.5 ps FWHM) and by comparing to the case of thicker foils which display longer durations associated with colder plasmas, we deduce that the observed emission is coming from the hottest area which is produced in the highest laser intensity zone. Moreover, time and spatially integrated spectra show, for thin foils, an absence of K_α emission (no cold K_α nor ionized states K_α) and consequently no lateral heat transport. This indicates furthermore that the thermal emission is confined to the hottest region of the interaction area. We also verify that, in the case of significant laser transmission through the foil, the transmitted visible spectra are heavily modulated as one expects in the presence of a rapidly decreasing plasma density [5].

Figure 2(a) shows the transmission rates through 3000 Å of preheated CH targets obtained in the 2ω configuration ($I\lambda^2 \sim 3 \times 10^{18}$ W cm^{-2} μm^2). The creation beam has 0.5–5 J of energy and the delay between the creation beam and the interaction beam varies from 0 to 200 ps. As the critical density at this wavelength ($\sim 4 \times 10^{21}$ cm^{-3}) is in the region of steep profile, l_c remains small ($\sim 2\ \mu$m) over the range of creation beam energy and delay used. The main parameter for the transmission is then the peak overdense density inferred from the fitted hydrodynamic simulations. These results clearly indicate high transmission through very overdense layers. Moreover, there is a high threshold in the interaction beam intensity in order to observe transmission, as illustrated in Fig. 2(b). Two different preformed plasmas are used: (i) at

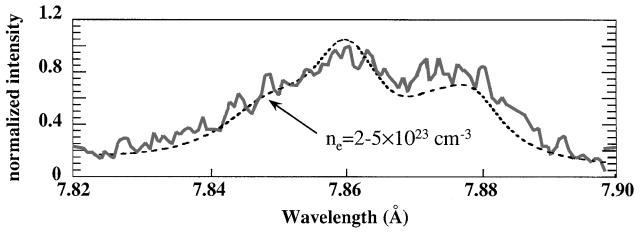

FIG. 1. Al Li-like spectrum produced by a 4.4×10^{18} W cm^{-2} μm^2 2ω shot focused on a 500 Å solid Al foil. The dotted curve is the corresponding calculation for an electron density of $2-5 \times 10^{23}$ cm^{-3}.

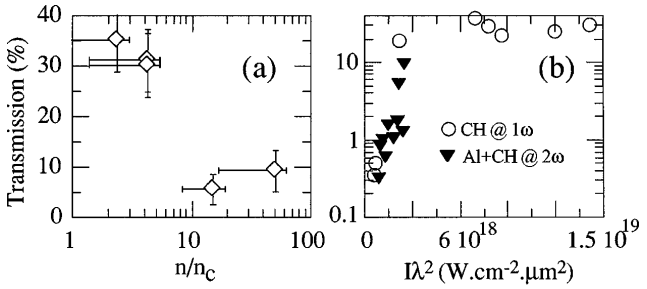

FIG. 2. Transmission rates of the short beam through preformed plasmas of (a) CH with $l_c \sim 2\ \mu$m and a variable peak density (2ω, $I\lambda^2 \sim 3 \times 10^{18}$ W cm^{-2} μm^2), (b) CH (1ω, circles) with $n_{\max}/n_c \geq 100$ and $l_c \sim 4\ \mu$m and Al and CH (2ω, triangles) with $n_{\max}/n_c \sim 45$ and $l_c \sim 1.5\ \mu$m.

1ω, we use a 3000 Å CH target, a 1–2 J creation beam, and $\Delta t = +100$ ps, leading to $n_{\max}/n_c$ above 100 and $l_c \sim 4\ \mu$m and (ii) at 2ω, we use a 1100 Å Al target coated on a 5800 Å CH film, a 2–5 J creation beam, and $\Delta t = +1$ ns, leading to $n_{\max}/n_c \sim 45$ and $l_c \sim 1.5\ \mu$m. The threshold intensity is below 10^{18} W cm^{-2} μm^2 [moderately relativistic, $a = (p_{\rm osc}/{\rm mc}) = (I_{\rm W\,cm^{-2}}\lambda_\mu^2/1.37 \times 10^{18})^{1/2} < 0.85$].

The 2ω high-contrast beam interaction with initially solid Al foils (no creation beam) ranging from 500 Å to 2 μm gives essentially the same results (transmission through highly overdense slabs and high intensity threshold). For all these foils, the inferred overdense peak density remains high (see Fig. 1) and quite constant. Thus the main control parameter is the thickness of the foil. Figure 3(a) shows the decrease of the transmission as the foil thickness increases. In the transmission regime, the absorption (estimated as the complement of the sum of reflection and transmission) is high (>50%), in good agreement with absorption measurements made using integrating spheres in the same 2ω configuration and with similar targets [15]. Through solid 0.15–0.3 μm of CH targets, we measure transmission rates ~2% at full beam intensity. Through solid foils, a high threshold in the interaction beam intensity is also found in order to observe transmission, as illustrated in Fig. 3(b) for 700 and 1000 Å

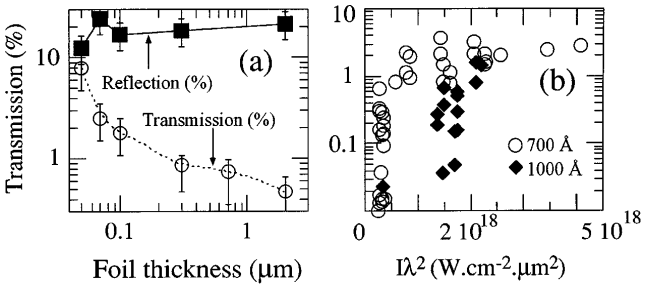

FIG. 3. Transmission-reflection rates of the 2ω beam through solid-density foils: (a) Al solid foils of variable thickness ($I\lambda^2 \sim 4 \times 10^{18}$ W cm^{-2} μm^2) and (b) 700 and 1000 Å of Al.

Al foils. The intensity threshold clearly increases as the foil thickness increases. This transition from opacity to transmission is also seen in the reflection rates. They are low [a (15–20)% plateau] when the transmission is high and conversely high (>90%) when there is no transmission. This latter result implies very low absorption at a steep interface [2].

Another observation that supports propagation through the entire foil is the rear imaging of the foil. A typical image of the intense short beam outcoming from a solid 0.3 μm CH foil is shown in Fig. 4(b). In Fig. 4(c), the plotted mean integrated energies show that it is indeed the intense part of this focused energy which mostly contributes to the beam transmission. Similar results are obtained in the case of Al solid foils.

The data presented in this Letter are clear indications of light propagation in very overdense plasmas and initially solid foils. However, their interpretation is not straightforward. The mechanisms most commonly associated with the electromagnetic penetration in overdense plasma are SIT and hole boring. The former occurs above an intensity such that $a \sim (n_e/n_c)$ [9]. One-dimensional PIC simulations done at $I\lambda^2 \sim 10^{19}$ W cm^{-2} μm^2 with a slightly overdense slab ($n_e = 1.5n_c$) show propagation at a velocity ~$0.2c$ through layers having a width 10–30 times the vacuum wavelength [9]. The classical description of the hole boring allows penetration in much denser plasmas but at a much lower velocity. It involves the ponderomotive force associated with the high intensity laser light which pushes the plasma electrons and ions at a velocity $u/c \sim a[(n_c/2n_e)(Zm_e/Am_i)]^{1/2}$ [10], where A is the atomic mass, m_i and m_e are, respectively, the nucleon and the electron mass, and Z is the effective charge

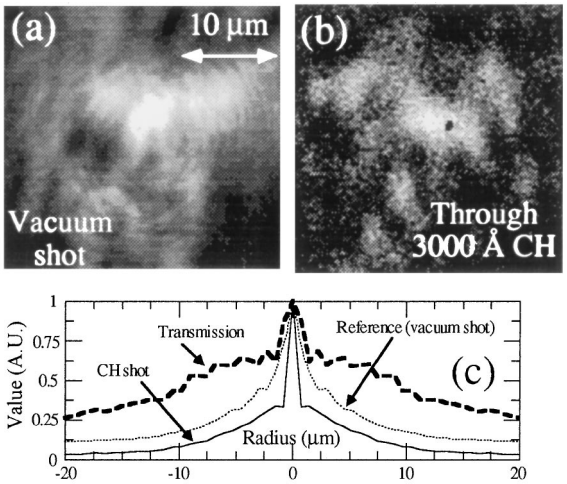

FIG. 4. Image of the focal spot: (a) calibration shot in vacuum and (b) on the rear side of a 0.3 μm solid CH foil, the 2ω beam ($I\lambda^2 \sim 5.6 \times 10^{18}$ W cm^{-2} μm^2) is seen to emerge from a small spot, and (c) normalized integrated energy inside a circular area of increasing radius for both shots and transmission (CH shot divided by the reference shot in vacuum).

state. Two-dimensional PIC and fluid simulations done with a semi-infinite step density $\leq 10 n_c$ and at $I\lambda^2 \sim 10^{19}$ W cm^{-2} μm^2 [10] are in agreement with this simple estimate for the penetration velocity. In addition, numerical simulations of the anomalous skin effect that allows enhanced penetration of laser fields in very overdense plasmas due to a nonlocal description of the conductivity predicts transmissions $<0.1\%$ for 500 Å of Al targets [16].

In order to discuss our results, we have to consider separately the preformed plasmas and the initially solid thin foils. The transmission regime with preformed plasmas could be the result of combined SIT and hole boring processes enhanced by the occurrence of self-focusing, in the underdense corona, that can significantly increase the laser intensity [17]. Relevance of these processes and the requirement of intense pulses to propagate through thick overdense preformed plasmas (12 μm of H at $50 n_c$ using a 10^{21} W cm^{-2} pulse) have been demonstrated using 2D PIC simulations [18]. However, through thin solid foils where x-ray spectroscopy indicates an initial density of $n_{\max}/n_c > 50$, these sole processes cannot describe our observations. First, we see transmission for values of intensities far below the corresponding SIT threshold. Moreover, on the contrary to the case of thick foils, the classical description of hole boring is inappropriate for thin foils. Indeed, as these thin foils are much more heated than the thick foils due to the hot electron return currents that interact over a long time with the beam [19], an outward ion flow is created that counters the hole boring pressure. Preliminary results from 2D Cartesian PIC simulations made with parameters similar to the experimental ones indicate rapid heating of the thin foil by these fast electrons crossing the foil back and forth, rapid expansion and density decrease to overcritical values where the plasma becomes relativistically transparent to the incident pulse. Using a beam with parameters $a = 2.7$, $\lambda = 1$ μm, 300 fs FWHM duration, a 4 μm FWHM focal spot, and a 0.1 μm, $n_e = 100 n_c$ initially cold foil, the simulation shows a 4.5% transmission (which can be attributed neither to pure SIT nor to hole boring), 45% reflection (in the focal cone), 30% absorption, and a broadened and modulated transmission spectrum, in good agreement with the experimental observations. We observe an effective density (n_e/γ) lowering below n_c that allows the beam propagation. The simulations were performed on 64 processors of a Cray/T3E.

We are thankful for the technical assistance of the P102-Castor staff at CEA Limeil and R. Caland, as well as D. Sznajderman at IPN-Orsay for providing the targets. We also thank T. W. Johnston, J. Meyer-ter-Vehn, and A. Pukhov for fruitful discussions, as well as Z. Jiang and O. Peyrusse for discussions and x-ray spectra calculations. The PIC simulations were performed using IDRIS, the CNRS computer facility.

[1] A. Akhiezer and R. Polovin, Sov. Phys. JETP **3**, 696 (1956); P. Kaw and J. Dawson, Phys. Fluids **13**, 472 (1970).
[2] E. Lefebvre and G. Bonnaud, Phys. Rev. E **55**, 1011 (1997), and references therein.
[3] S. Vukovic and R. Dragila, J. Opt. Soc. Am. B **3**, 1585 (1986).
[4] M. Zepf *et al.*, Phys. Plasmas **3**, 3242 (1996).
[5] H. Nishimura *et al.*, Jpn. J. Appl. Phys. **22**, L786 (1983); R. Kodama *et al.*, Phys. Rev. Lett. **77**, 4906 (1996).
[6] N. Blanchot *et al.*, Opt. Lett. **20**, 395 (1995).
[7] M. Tabak *et al.*, Phys. Plasmas **1**, 1626 (1994).
[8] J. Fuchs *et al.*, Phys. Rev. Lett. **80**, 1658 (1998).
[9] S. Guérin *et al.*, Phys. Plasmas **3**, 2693 (1996).
[10] S. C. Wilks *et al.*, Phys. Rev. Lett. **69**, 1383 (1992); S. Omel'chenko *et al.*, Quantum Electron. **26**, 565 (1996); A. Pukhov and J. Meyer-ter-Vehn, Phys. Rev. Lett. **79**, 2686 (1997).
[11] S. Jacquemot and A. Decoster, Laser Part. Beams **9**, 517 (1991).
[12] P. Mora and J. F. Luciani, Laser Part. Beams **12**, 387 (1994).
[13] J. C. Kieffer *et al.*, J. Opt. Soc. Am. B **13**, 132 (1996).
[14] O. Peyrusse *et al.*, J. Phys. B **26**, L511 (1993); D. Gilles, in *Spectral Line Shapes*, edited by L. Frommhold and J. W. Keto (American Institute of Physics, New York, 1990), Vol. 6, p. 48.
[15] T. Feurer *et al.*, Phys. Rev. E **56**, 4608 (1997).
[16] J. P. Matte and K. Aguenaou, Phys. Rev. A **45**, 2558 (1992).
[17] A. Pukhov and J. Meyer-ter-Vehn, Phys. Rev. Lett. **76**, 3975 (1996).
[18] B. F. Lasinski and A. B. Langdon, in *Proceedings of the 27th Anomalous Absorption Conference, Vancouver, Canada, 1997* (The University of British Columbia, Vancouver, 1997), p. 202.
[19] E. Lefebvre, Ph.D. dissertation, Paris XI University, 1997 (see Sects. B.V and C.III).